

Low-Profile and Small Capacitively Fed VHF Antenna

Yaakoub Taachouche^{1, *}, Franck Colombel¹, Mohamed Himdi¹, and Antoine Guenin²

Abstract—A low profile, compact antenna operating around 162 MHz with omnidirectional vertically polarized radiation is proposed. The antenna is a short monopole capacitively coupled to short-end quarter-wavelength printed line optimized at 162 MHz for Automatic Identification System (AIS) application. The antenna dimensions are less than $\lambda/185$ in height and $\lambda/20$ in lateral dimension, and the small size of antenna provides a narrow band of 0.34% and gain of -11.6 dBi. The simulated and measured results are in good agreement.

1. INTRODUCTION

The recent developments of wireless communication technologies increase the demand of multisystem applications. One of the major challenges is the integration of antennas inside the device including many systems in a limited area. For example, several standards are included in the mobile handset, and as a consequence the need to embed an antenna operating in the UHF band becomes a weak part. For marine applications, the situation is similar because there are usually many radio communication systems close to each other. In this field of interest, the Automatic Identification System (AIS) is an automatic tracking system used on ships and by vessel traffic services to identify and locate vessels by electronically exchanging data [1, 2]. For terrestrial AIS application, an omnidirectional coverage is requested and the most commonly used antenna is a monopole operating at 162 MHz. The goal of this paper is to propose a compact antenna as an alternative to the historical monopole in order to improve the integration capability of the whole system.

In the past few years, the monopoles and their variations have been largely investigated. A wide range of shapes has been studied such as square, circular or semi-elliptical monopoles [3, 4]. All these structures are small and thin but if one uses these basic ideas for AIS applications, the antenna is still bulky. It is thus recommended to propose a low-profile vertically polarized antenna which is able to provide an omnidirectional coverage.

A large variety of design has been studied to reduce the vertical profile of monopole antennas. In [5], the performances of the Hilbert curve fractal monopole are presented. For an operating frequency close to 165 MHz, the antenna's height is approximately 0.125λ . In [6], a small meander line dipole loaded with a high permittivity dielectric ($\epsilon_r = 20$) is presented. As a result, its size is reduced to $0.05\lambda \times 0.04\lambda$, but the gain is close to -6.4 dBi. In [7], a monopole coupled loop antenna (MCLA) is studied. The antenna operates around 450 MHz and provides a quasi-unidirectional radiation pattern and a gain close to -3.3 dBi. The antenna height is reduced to $\lambda/37$. In [8], a vertically polarized antenna operating around 460 MHz is presented; it is $\lambda/40$ high and $\lambda/10$ wide. The measured gain is close to -3.1 dBi.

The use of capacitive coupling as an effective way to design electrically small antennas that can operate at the serial resonance frequency is presented in [9].

Received 11 February 2016, Accepted 21 March 2016, Scheduled 12 May 2016

* Corresponding author: Yaakoub Taachouche (yaakoub.taachouche@univ-rennes1.fr).

¹ IETR (Institut d'Electronique et de Telecommunications de Rennes), UMR-CNRS 6164, Campus de Beaulieu, 263 avenue du General Leclerc, Rennes 35042, France. ² Photospace, Melun, France.

In this paper, a small, low profile antenna with omnidirectional vertically polarized radiation is presented. The imposed specifications dimensions of the antenna must not exceed 10 mm in height and 90 mm in diameter.

Using the capacitive coupling effect, we propose a design based on a short monopole coupled with a folded short-ended quarter wavelength line. The design of this antenna is presented in Section 2 followed with a theoretical and parametric studies in Section 3. In Section 4, the simulations and measurements are compared and discussed.

2. ANTENNA DESIGN

As depicted in Fig. 1, the folded printed line is short circuited on one side and fed with a coupling effect on the other side. The feeding system is built with a very short monopole (10 mm) connected on its top part to an isolated printed disk and coupled through a very thin gap to the folded printed line.

The printed antenna is built on a 0.8 mm thick dielectric substrate (Neltec NX9300, $\epsilon_r = 3$, $\tan \delta = 0.0023$) and placed 10 mm above the metallic plane. The substrate is supported above the ground plane by a spacer foam (Rohacell HF51, $\epsilon_r = 1.07$). The total length of the folded printed line starting from the short circuit to the feeding point is close to $\lambda/4$ where λ is the wavelength at the operating frequency.

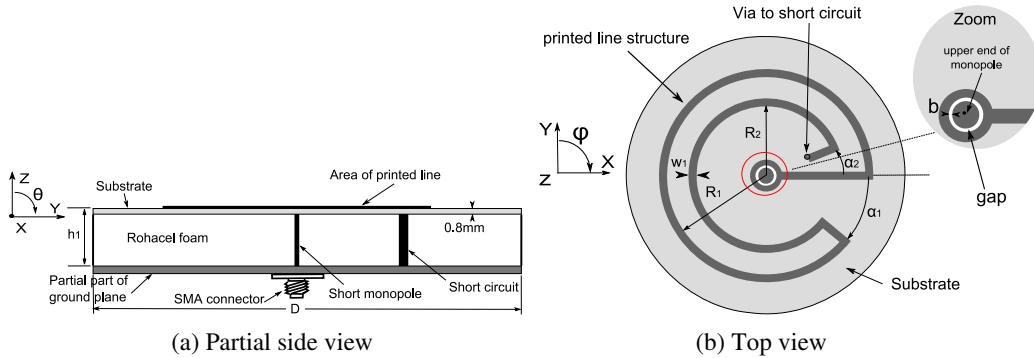


Figure 1. Geometry of the low-profile proposed antenna.

R_1 and R_2 are the radius of the inner and the outer loops of the folded printed line, respectively. w_1 is the line's width, b is the gap's width, α_1 and α_2 are the angles that define the length of the folded line, $D = 90$ mm is the antenna's diameter and $h_1 = 10$ mm the height between the antenna and the ground plane. In order to consider ohmic loss, the conductivity of copper is used in all metallic traces and vertical pins in the simulation software HFSS.

3. THEORETICAL AND PARAMETRIC STUDIES

Based on the design presented in Fig. 1 we propose an equivalent circuit which models the antenna. The equivalent circuit is shown in Fig. 2 and can be split into the following parts:

- The short monopole and the short pin are modeled with a serial inductor and resistance.
- The gap between the top of the short monopole and the short-ended quarter wavelength printed line is modeled with a π -network made with a capacitor as suggested in [10, 11]. Two parallel capacitors C_{p1} and C_{p2} represent the terminal capacitances of the two microstrip sections and the serial capacitance C_p represents the gap.
- The short-ended microstrip line is modeled by a quarter wavelength transmission line operating at 162 MHz.

Figure 3 shows the agreement between the electromagnetic and the circuit simulations for imaginary and real parts of the input impedance with a slight frequency shift.

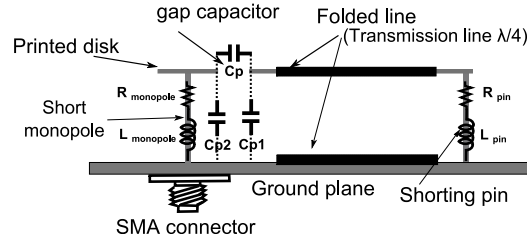


Figure 2. Equivalent circuit model of the antenna.

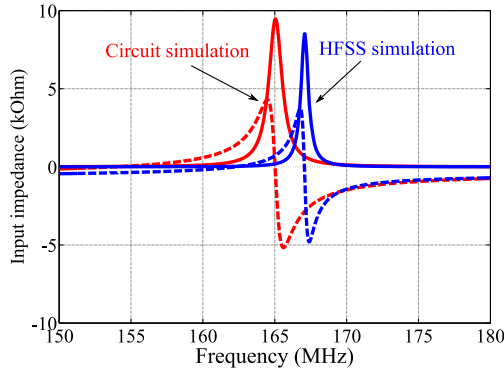


Figure 3. Input impedance of the antenna obtained with circuit and HFSS electromagnetic simulations (— Real, - - - Im) ($C_p = 1.1$ pF, $C_{p1} = 100$ pF, $C_{p2} = 1$ pF, $L_{pin} = L_{monopole} = 27$ nH, $R_{pin} = R_{monopole} = 0.03 \Omega$).

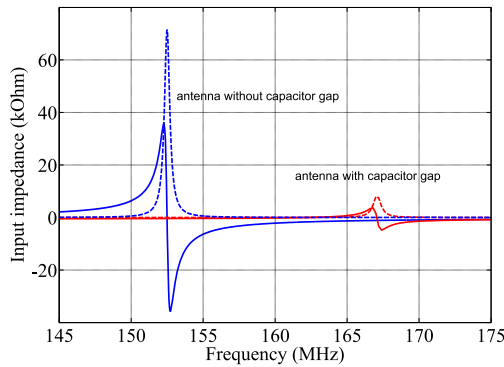


Figure 4. HFSS simulation of the effect of the capacitor gap on the input impedance (--- Real, — Im).

3.1. Effect of the Gap

Figure 4 shows the effect of the capacitor gap on the input impedance of the antenna. Without the gap, the antenna presents a high resistance and a high reactance around the resonance frequency because the structure is equivalent to a short-ended quarter wavelength transmission line.

Based on the Fig. 4, the introduction of the gap induces the addition of the capacitances (C_{p1} , C_{p2} , C_p) as it has been explained at the beginning of this section. It results in a reduction of the high Q -factor of the resonator with slight frequency shifts and a translation of the reactance curve vertically downward.

By varying the gap’s width (Fig. 5(a)), we can adjust vertically the reactance of the antenna and choose a resonance frequency to provide a serial resonance (reactance = 0). When the gap’s width ‘ b ’ varies from 0.1 mm to 1 mm, the input impedance varies from 13Ω to 80Ω in the 154–166 MHz range (see Fig. 5(b)).

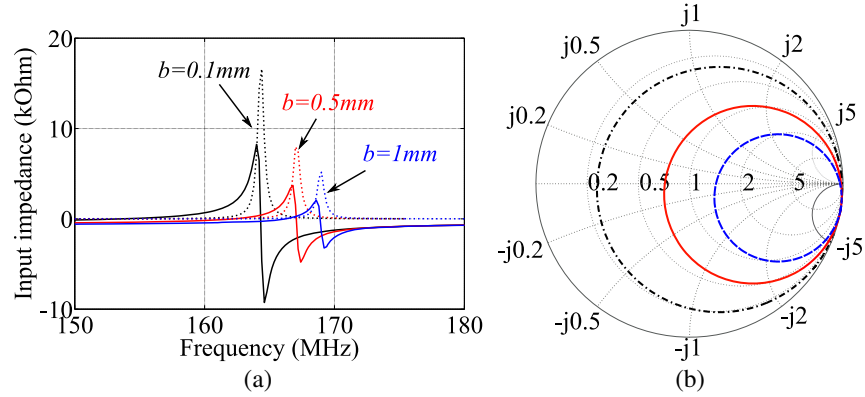


Figure 5. (a) Simulated real and imaginary parts of the input impedance versus b (\cdots Real, $—$ Im). (b) Simulated input impedance of the proposed antenna versus b ($---$ 0.1 mm, $—$ 0.5 mm, $---$ 1 mm).

3.2. Length of the Folded Quarter Wavelength

We have seen in the previous section that the short-ended quarter wavelength printed line has a high Q -factor resonator. The length's variation of this line provides a frequency shift without a significant change on the reactance and resistance magnitude.

By adjusting the length parameters (R_1 , R_2 , α_1 , α_2) of the printed line, we could tune the resonant frequency of the antenna. In this case, the impedance has a small variation around the desired value and the antenna is matched.

As an example, we present in Fig. 6 the variation of the S_{11} versus R_1 . In our study, R_1 varies from 33 to 42 mm and when R_1 increases, the total length of the folded printed line also increases. As a consequence, the resonant frequency decreases from 193 MHz to 157 MHz.

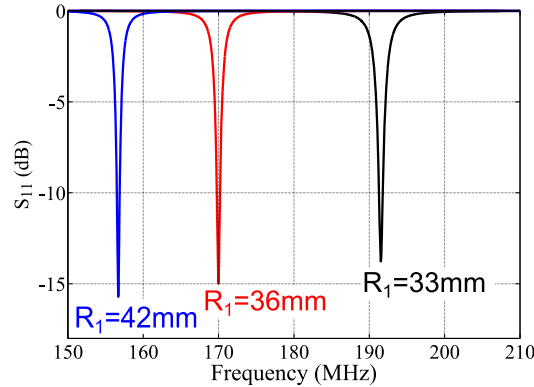


Figure 6. Simulated return loss of the proposed antenna versus R_1 ($b = 0.5\text{ mm}$).

3.3. Radiation Patterns

We have calculated the radiation patterns at the resonant frequency. As depicted in Fig. 7(a), we obtained an E -plane radiation patterns (E_θ component) similar to those provide by a monopole antenna with a limited ground plane. In our case, the ground plane ($D = 90\text{ mm}$) is small relatively to the wavelength. Thus, the radiating power is almost the same in both sides of the antenna.

We have also analyzed the behavior of the antenna in order to understand which part of the antenna really provides a radiating contribution. The currents drawn on the antenna in Fig. 7(b) give a schematic view of the surface currents on the folded printed line. On the inner and on the outer circles of the folded printed line, the currents have opposite directions but not the same magnitude.

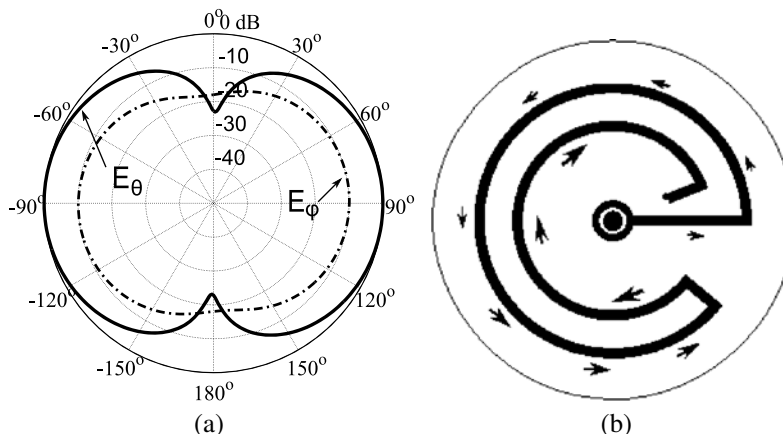


Figure 7. (a) Simulated radiation pattern in E -plane (E_ϕ and E_θ) of the proposed antenna ($h_1 = 10$ mm) at $\phi = 0^\circ$. (b) Schematic view of currents directions on the folded printed line.

Hence, they cancel partially themselves and they contribute to the high level of cross polarization (E_ϕ component). The electric current flowing on the short monopole of the antenna is the main contributor of the vertically polarized radiation.

We have calculated a gain of -12.8 dBi with an efficiency of 3.5%. This low gain is due to the antenna size and the ohmic loss in the thin width of the printed line. We can estimate this antenna efficiency by the following computation. From [12], the radiation resistance and loss resistance of an infinitesimal monopole is equal to $R_{RM} = 0.023 \Omega$ and $R_{LM} = 0.01 \Omega$, respectively. We have also calculate a loss resistance $R_{LTL} = 0.48 \Omega$ for the printed line. The loss resistance of the antenna is $R_{LA} = R_{LTL} + R_{LM}$. The radiation efficiency can be estimated as:

$$\rho_{new} = R_{RM} / (R_{RM} + R_{LN}) = 4.5\% \quad (1)$$

The estimate and simulated efficiency are in good agreement. The gain could be improved by increasing the height h_1 and the width w_1 .

To conclude this parametric study, we underline that the proposed antenna has a few degrees of freedom very useful to match it for narrow band vertically polarized VHF applications.

4. EXPERIMENTAL RESULTS

As mentioned in the introduction, our goal is to propose a very compact antenna for the narrow band Automatic Identification System (AIS) used for marine applications. Based on the previous results, an antenna has been optimized theoretically at 162 MHz. The height h_1 (10 mm) has not been optimized because it was a constraint of our project. The optimized dimensions of the antenna presented in Fig. 1 are : $R_1 = 38$ mm, $R_2 = 27$ mm, $D = 90$ mm, $w_1 = 3$ mm, $\alpha_1 = 15^\circ$, $\alpha_2 = 18^\circ$, $h_1 = 10$ mm and $b = 0.5$ mm. The picture of the proposed antenna is shown in Fig. 8.

In Fig. 9, we present the simulated and the measured return loss. The measured resonance frequency is 162.85 MHz with 0.5 MHz of -10 dB return loss bandwidth, we have a slight frequency shift of 0.52% compared with operating frequency of 162 MHz. We can adjusting the resonance frequency and overcome the shift frequency by Adjusting the parameters α_1 or R_1 .

We have measured the radiation pattern in an outside test range. As depicted in Fig. 10, to reduce the feed cable influence, the antenna has been installed on a limited square ground plane 1 m \times 1 m, 1.65 m above the soil. In the calculation radiation pattern, the soil is characterized by an infinite ground plane with the following characteristics (Conductivity $\sigma = 10^{-2}$ S/m, $\epsilon_r = 15$).

The radiation patterns are plotted in Fig. 11. The E -plane radiation patterns are symmetrical and similar to those provided by a vertically polarized monopole antenna. The ripples seen on these patterns are due to the earth effects which were difficult to consider in simulation with a very good accuracy.



Figure 8. Photograph of the fabricated antenna.

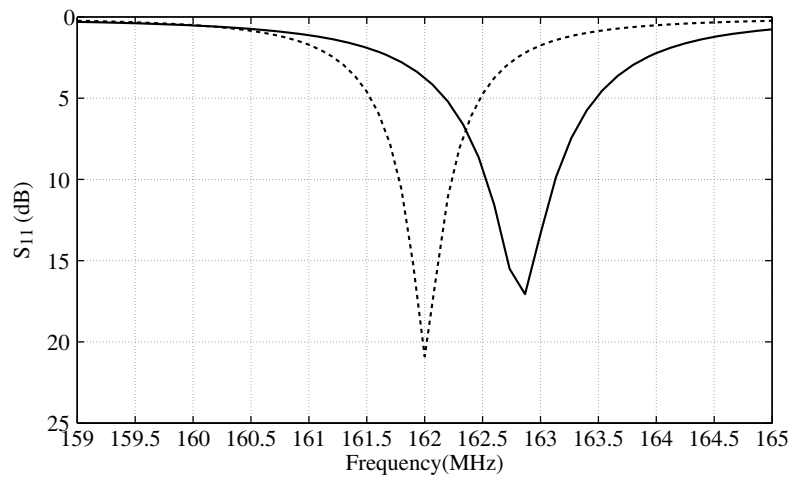


Figure 9. Measured and simulated return loss versus frequency of the proposed antenna (— measured, --- simulated).

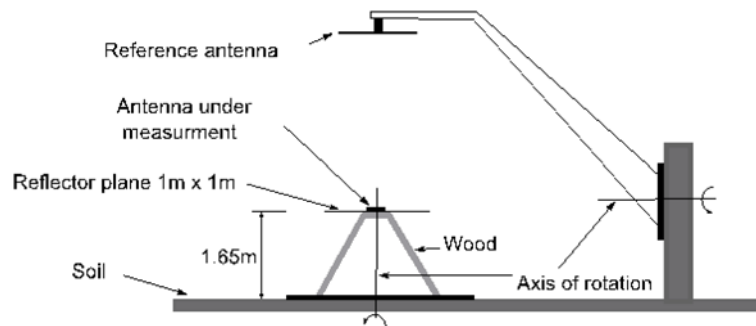


Figure 10. Measurement radiation pattern test range.

The simulated and measured gains of the antenna are close to -10.5 dBi and -11.6 dBi, respectively. The gain values pointed out here correspond to the maximal gain obtained in the E -plane at 162 MHz. We measured an efficiency equal to 3.4%.

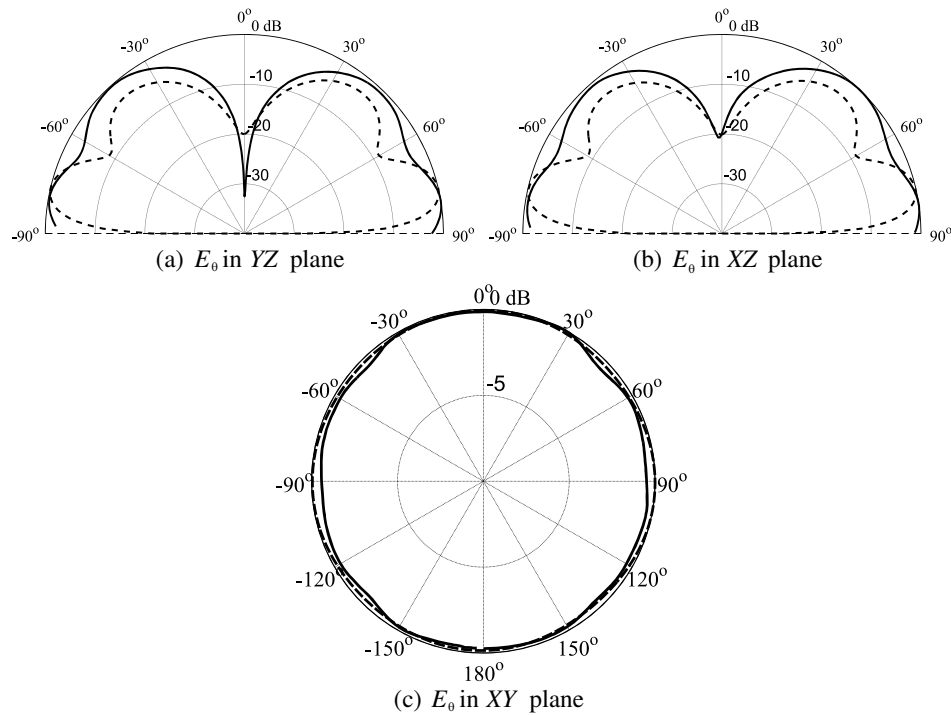


Figure 11. Measured and simulated normalized radiation pattern in E -plane and H -plane of the proposed antenna (— measured, --- simulated) at 162 MHz.

5. CONCLUSION

A very compact omnidirectional antenna operating at 162 MHz has been investigated, for AIS marine application. The antenna is based on a folded printed line fed by a very short monopole with a coupling effect. Regarding the operating frequency of 162 MHz, the antenna size is less than $\lambda/185$ high and $\lambda/20$ wide. Simulations and measurements are in good agreement, and the radiation patterns in the E -plane are similar to those provided by a monopole. The measured gain of the antenna is close to -11.6 dBi and is suitable for the need of our application. Techniques to improve the gain by increasing the height of antenna and the width of the quarter wavelength line will be investigated in the future studies.

ACKNOWLEDGMENT

The authors warmly thank L. Lz and J. Aussant from TDF for their participation in the measurements.

REFERENCES

1. Cervera, M. A. and A. Ginesi, "On the performance analysis of a satellite-based AIS system," *SPSC 2008. 10th International Workshop on Signal Processing for Space Communications, 2008*, 1–8, Rhodes Island, 2008.
2. Dousset, T., C. Renard, H. Diez, J. Sarrazin and A. C. Lepage, "Compact patch antenna for automatic identification system (AIS)," *2012 15th International Symposium on Antenna Technology and Applied Electromagnetics (ANTEM)*, 1–5, Toulouse, 2012.
3. Ammann, M. J. and Z. N. Chen, "Wideband monopole antennas for multi-band wireless systems," *IEEE Antennas Propag. Mag.*, Vol. 52, No. 2, 146–150, April 2003.
4. Tang, M.-C., T. Shi, and R. W. Ziolkowski, "Planar ultrawideband antennas with improved realized gain performance," *IEEE Transactions on Antennas and Propagation*, Vol. 64, No. 1, 61–69, January 2016.

5. Best, S. R., "A comparison of the performance properties of the Hilbert curve fractal and meander line monopole antennas," *Microw. Opt. Technol. Lett.*, No. 35, 258–262, 2002.
6. Michishita, N. and Y. Yamada, "High efficiency achievement by material loading for a piled type small meander line antenna," *IEEE AP-S Int. Symp*, Vol. 1B, 492–495, July 2005.
7. Taachouche, Y., F. Colombel, and M. Himdi, "Meandered monopole coupled loop antenna," *2012 6th European Conference on Antennas and Propagation (EUCAP), Prague*, 3005–3008, 2012.
8. Hong, W. B. and K. Sarabandi, "Low-profile, multi element, miniaturized monopole antenna," *IEEE Transactions on Antennas and Propagation*, Vol. 57, No. 1, 72–80, January 2009.
9. Maema, H. and T. Fukusako, "Radiation efficiency improvement for electrically small and low-profile antenna by stacked elements," *IEEE Antennas and Wireless Propagation Letters*, Vol. 13, 305–308, 2014.
10. Cho, Y. K., G. H. Son, G. S. Chae, L. H. Yun, and J. Hong, "Improved analysis method for broadband rectangular microstrip antenna geometry using E-plane gap coupling," *Electronics Letters*, Vol. 29, No. 22, 1907–1909, 28 October 1993.
11. Kirschning, M., R. H. Jansen, and N. H. L. Koster, "Measurement and Computer-Aided Modeling of Microstrip Discontinuities by an Improved Resonator Method," *1983 IEEE MTT-S International Microwave Symposium Digest*, 495–497, May 31 1983–June 3, 1983.
12. Balanis, C. A., *Antenna Theory: Analysis and Design*, 3rd edition, John Wiley & Sons, 2005.